Weierstraß-Institut

für Angewandte Analysis und Stochastik

Leibniz-Institut im Forschungsverbund Berlin e. V.

Uncertainty quantification for hysteresis operators and a model for magneto-mechanical hysteresis

Olaf Klein

submitted: April 11, 2016

Weierstrass Institute
Mohrenstr. 39
10117 Berlin
Germany
E-Mail: Olaf.Klein@wias-berlin.de

Abstract

Many models for magneto-mechanical components involve hysteresis operators. The parameter within these operators have to be identified from measurements and are therefore subject to uncertainties. To quantify the influence of these uncertainties, the parameter in the hysteresis operator are considered as functions of random variables. Combining this with the hysteresis operator, we get new random variables and we can compute stochastic properties of the output of the model. For two hysteresis operators corresponding numerical results are presented in this paper. Moreover, the influence of the variation of the parameters in a model for a magneto-mechanical component is investigated.

1   Introduction

Hysteresis operators as in [1, 8, 9, 10, 12] are used in many models for magneto-mechanical components, see, e.g., [10, 3, 4, 5]. The parameter within these operators have to be identified from measurements, and there are deviations in the measurements. In addition, parameters being identified for some sample devices are used to model other devices. Moreover, the observable macroscopic initial state may be generated by several microscopic initial states which cannot (easily) be identified.

The parameters in the *hysteresis operators* used to model hysteresis effects are therefore also subject to uncertainties. To quantify the influence of these uncertainties, the parameter for the hysteresis operators, including the (internal) initial states, are considered as functions of random variables. Combining this with the hysteresis operators, we get new random variables and we can compute stochastic properties of the output of the model, e.g. the expectation value and the variance of the new random variable. Moreover, we can apply methods of *uncertainty quantification*, see, e.g., [11], to quantify the influence of the uncertainties in the parameters on the output of the hysteresis operators and of the considered model.

2   Hysteresis operators

2.1   Definition

Let $T > 0$ denote some final time.

Definition 2.1. Let $\mathrm{Map}[0, T]$ be the set of all functions from $[0, T]$ to $\mathbb{R}$, let $C[0, T]$ be the set of at continuous functions in $\mathrm{Map}[0, T]$.

Following [1, 9, 10, 12], we define:

Definition 2.2. Let $\mathcal{H} : C[0, T] \to \mathrm{Map}[0, T]$ be given.

- $\mathcal{H}$ is denoted as *hysteresis operator* if and only if $\mathcal{H}$ is rate-independent and causal.

- $\mathcal{H}$ is denoted as *rate-independent* if and only if for all $v \in C[0, T]$ and for all $\alpha : [0, T] \to [0, T]$ being continuous and increasing (not necessary strictly increasing), with $\alpha(0) = 0$ and $\alpha(T) = T$ it holds:

$$\mathcal{H}[v \circ \alpha](t) = \mathcal{H}[v](\alpha(t)), \quad \forall t \in [0, T]. \tag{1}$$

- $\mathcal{H}$ is denoted as *causal* if and only if for all $v_1, v_2 \in C[0, T]$, and for all $t \in [0, T]$ it holds that:

  If $v_1(\tau) = v_2(\tau)$ for all $\tau \in [0, t]$ then it follows that $\mathcal{H}[v_1](t) = \mathcal{H}[v_2](t)$.

2.2 Example: the play operator

Following [1, 8, 9, 12], we consider for all *yield limits* $r \geq 0$ and all *initial state* w_0 the *play operator* $\mathcal{P}_r[w_0, \cdot]$. This operator maps $u \in C[0, T]$ to $\mathcal{P}_r[w_0, u] \in C[0, T]$ and it holds

$$\mathcal{P}_r[w_0, u](0) = \max\left(u(0) - r, \min\left(u(0) + r, w_0\right)\right)$$

$$\mathcal{P}_r[w_0, u](t) = \begin{cases} \max\left(\mathcal{P}_r[w_0, u](t_0), u(t) - r\right), \text{ if } u \text{ is} \\ \qquad \text{increasing on } [t_0, t], \\ \min\left(\mathcal{P}_r[w_0, u](t_0), u(t) + r\right), \text{ if } u \text{ is} \\ \qquad \text{decreasing on } [t_0, t]. \end{cases}$$

for all $t_0, t \in [0, T]$ with $t_0 < t$ such that u **is monotone on** $[t_0, t]$.

For an input function u increasing from 0 to 1.5, decreasing afterwards to -2.5, increasing then to 4, decreasing to -1 afterwards, increasing to 6, decreasing to 1 and finally increasing to 4, the evolution of $u(t)$, of the yield boundaries $u(t) - r$ and $u(t) + r$ for the yield limit $r = 2$, and of the output of the play-operator $\mathcal{P}_2[0, u](t)$ are shown in Figure 1. The corresponding pairs $(u(t), \mathcal{P}_2[0, u](t))$ are shown in the input-output diagram in Figure 2.
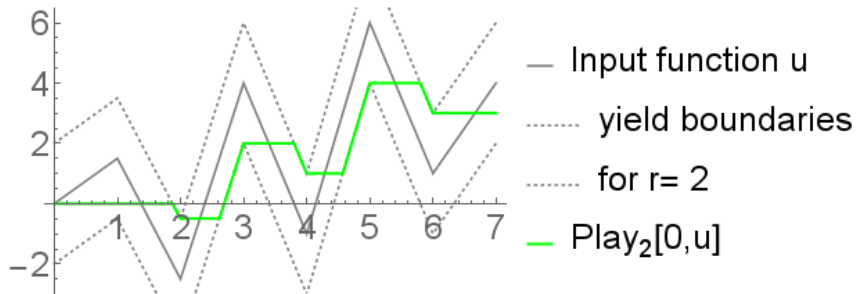

Figure 1: Evolution of the considered input function u, of the yield boundaries $u(t) - 2$ and $u(t) + 2$ for the yield limit $r = 2$, and of the output of the play-operator $\mathcal{P}_2[0, u](t)$.
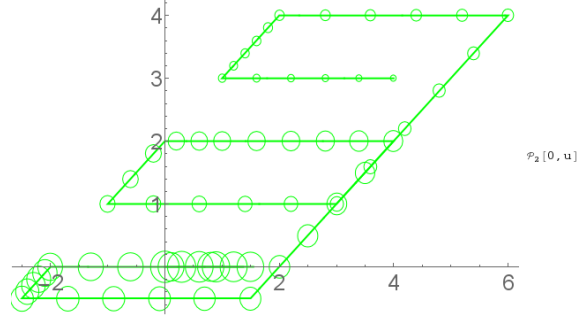
2

Figure 2: Input-output diagram, showing $(u(t), \mathcal{P}_2[0, u](t))$ for u as in Figure 1. The size of the circles decreases with increasing time t.

2.3 Dependence of the output of the play operator on the yield limit

Now, we consider an input function u that increases from 0 to 2, decreases afterwards to -3.5, increases afterwards to 4, decreases afterwards to 1.5, and increases finally to 6. For this input function u, the evolution of u, of the output $\mathcal{P}_r[0, u]$ of the play operator with initial state 0 and yield limits $r \in \{1, 1.5, 2, 2.5, 3\}$ are shown in Figure 3. The corresponding input-output diagrams are presented in Figure 4.
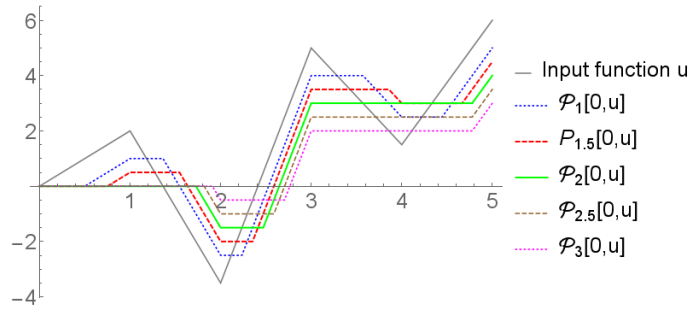

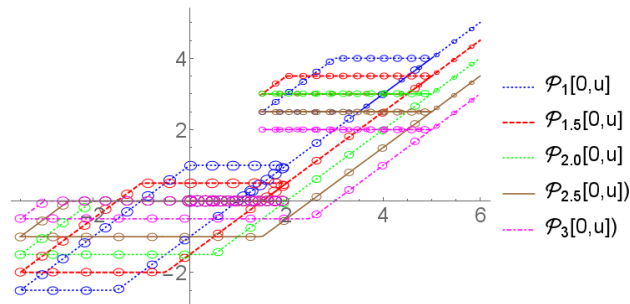Figure 3: Evolution of the input function u and of $\mathcal{P}_r[0, u]$ for $r \in \{1, 1.5, 2, 2.5, 3\}$.

Figure 4: Input-output diagram, showing $(u(t), \mathcal{P}_r[0, u](t))$ for u and and $\mathcal{P}_r[0, u]$ as in Figure 3. The size of the circles decreases with increasing time t.

3 Yield limit as random variable

3.1 As parameter interpreted random variable

As a first example for an uncertain parameter, we consider a situation, where the yield limit is not certainly known; but is only known to be approximately equal to 2.

To model this situation, the yield limit is interpreted as the value of a *random variable*, see, e.g., [6]. To ensure that this random variable does not attain negative values, it is generated from the normal distribution (see, e.g., [6]) $N(2, 0.5)$ with mean 2 and variance 0.5 by ignoring $(-\infty, 0)$ and performing an appropriate rescaling, leading to the following *probability density function ρ_R* of the considered random variable R:

$$\rho_R(r) = \frac{1}{C_1} \begin{cases} e^{-\frac{1}{2}(r-2)^2 \frac{1}{0.5}}, & \text{if } r \geq 0, \\ 0, & \text{if } r < 0, \end{cases} \tag{2}$$

with

$$C_1 = \int_0^\infty e^{-\frac{1}{2}(r-2)^2 \frac{1}{0.5}} \, dr \,. \tag{3}$$

The density function ρ_R is presented in Figure 5.
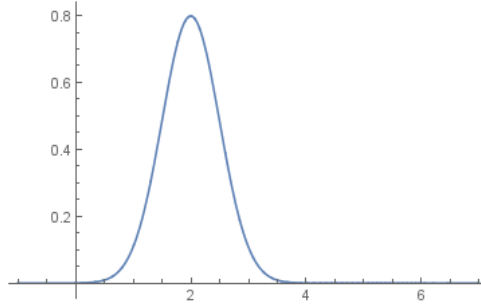

Figure 5: The probability density function ρ_R of the random variable R representing the yield limit r.

3.2 Generated random variable, expectation value and variance

Considering the yield limit as random variable and evaluation the play operator, we generate new random variables:

Definition 3.1. For every $w \in \mathbb{R}$, for every continuous input function $v : [0, T] \to \mathbb{R}$ and for every $t \in [0, T]$ it holds: $\mathcal{P}_R[w, v](t)$ denotes the random variable created as composition of the mapping $[0, \infty) \ni r \mapsto \mathcal{P}_r[w, v](t)$ with R.

Since $\mathcal{P}_R[w, v](t)$ as in Definition 3.1 is a random variable, we can compute its *expectation value* $\mathbb{E}\left(\mathcal{P}_R[w, v](t)\right)$ and its *variance* $\text{Var}\left(\mathcal{P}_R[w, v](t)\right)$, see, e.g. [6]. Thanks to the construction of $\mathcal{P}_R[w, v](t)$ as composition of R with the mapping introduced in Definition 3.1, it

4

follows that for w, v, t as in this definition it holds:

$$\mathbb{E}\left(\mathcal{P}_R[w,v](t)\right) = \int_0^\infty \mathcal{P}_r[w,v](t)\rho_R(r)\,\mathrm{d}r\,, \tag{4}$$

$$\mathsf{Var}\left(\mathcal{P}_R[w,v](t)\right) = \int_0^\infty \left(\mathcal{P}_r[w,v](t) - \mathbb{E}\left(\mathcal{P}_R[w,v](t)\right)\right)^2 \rho_R(r)\,\mathrm{d}r\,. \tag{5}$$

Considering for fixed $w \in \mathbb{R}$ the operator defined by mapping $v \in C[0,T]$ to the function $\mathbb{E}\left(\mathcal{P}_R[w,v](\cdot)\right) \in C[0,T]$ that maps $t \in [0,T]$ to $\mathbb{E}\left(\mathcal{P}_R[w,v](t)\right)$, one realizes easily that this operator corresponds to a Prandtl-Ishlinskiĭ operator as it is considered for example in [1, 8, 9, 12].

3.3 Example for the evolution of expectation value and variance

Considering the input function u as in Section 2.3, the evolution of u, of $\mathcal{P}_2[0,u]$, of the expectation value $\mathbb{E}\left(\mathcal{P}_R[0,u](\cdot)\right)$, and of the variance $\mathsf{Var}\left(\mathcal{P}_R[0,u](\cdot)\right)$ are presented in Figure 6. As one can observe, the output of the $\mathcal{P}_2[0,u](t)$ and of $\mathbb{E}\left(\mathcal{P}_R[0,u](t)\right)$, are almost equal on some subintervals of $[0,T]$, but are different on the remaining part of $[0,T]$. The corresponding input-output diagrams for u and $\mathcal{P}_2[0,u]$ and for u and $\mathbb{E}\left(\mathcal{P}_R[0,u](\cdot)\right)$ are presented in Figure 7.
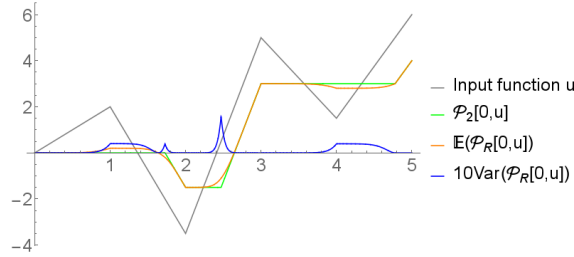

Figure 6: The evolution of the input function u, of $\mathcal{P}_2[0,u](t)$, of $\mathbb{E}\left(\mathcal{P}_R[0,u](t)\right)$, and of 10 times $\mathsf{Var}\left(\mathcal{P}_R[0,u](t)\right)$.

4 An example for an operator with internal states

4.1 The sum of two play operators

To construct a simple example of an operator with internal states, such that different sets of internal states can generated the same output for the operator, we consider the sum of play operators. Defining for the *initial state* $w \in \mathbb{R}$ the hysteresis operator $\mathcal{H}[w,\cdot] : C[0,T] \to C[0,T]$ by

$$\mathcal{H}[w,v](t) := \mathcal{P}_4[w,v](t) + \mathcal{P}_2[-w,v](t), \quad \forall t \in [0,T],\ v \in C[0,T], \tag{6}$$
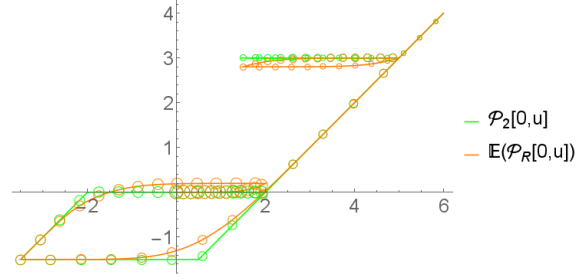
Figure 7: Input-output diagram, showing $\big(u(t), \mathcal{P}_2[0, u](t)\big)$ and $\big(u(t), \mathbb{E}\left(\mathcal{P}_R[0, u](t)\right)\big)$ for u as in Figure 6. The size of the circles decreases with increasing time t.

it follows that $\mathcal{P}_4[w, v]$ and $\mathcal{P}_2[-w, v]$ are *internal states* of $\mathcal{H}$.

It holds for all $w \in \mathbb{R}$ and all $v \in C[0, T]$ with $v(0) = 0$ that $\mathcal{H}[w, v](0) = 0$ if and only if $w \in [-2, 2]$, i.e. by considering the value of $\mathcal{H}[w, v](0)$ we can not determine uniquely the value of the initial state w or the initial values $\mathcal{P}_4[w, v](0)$ and $\mathcal{P}_2[-w, v](0)$ of the internal states.

4.2 Examples for the output of the sum of two play operators

Considering an input function u that increases from 0 to 2, decreases afterwards to -4 and increases to 5 and combining it with initial states w in $\{-2, -1, 0, 1, 2\}$, we get the evolutions shown in Figure 8, and the input-output diagrams in Figure 9.
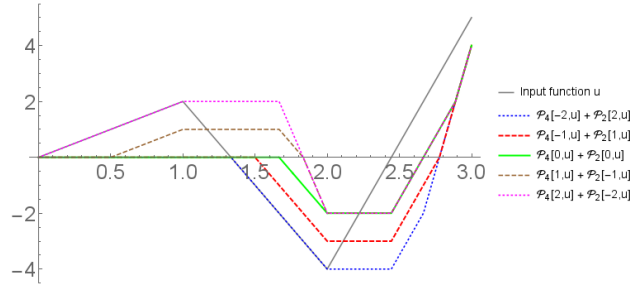

Figure 8: Evolution of the input function u and of $\mathcal{H}[w, u] = \mathcal{P}_4[w, u] + \mathcal{P}_2[-w, u]$ for w in $\{-2, -1, 0, 1, 2\}$.

4.3 Initial state as random variable

As a further example for an uncertain parameter, we consider a situation, where the initial state w is only known to be approximately equal to 0 and satisfies $\mathcal{H}[w, u] = 0$ for u as in Section 4.2. Hence, the initial state is interpreted as the value of a random variable generated from the standard normal distribution (see e.g. [6]) $N(0, 1)$ with mean 0 and variance 1 by ignoring $(-\infty, -2)$ and $(2, \infty)$ and rescaling. By doing this, we generate the following probability
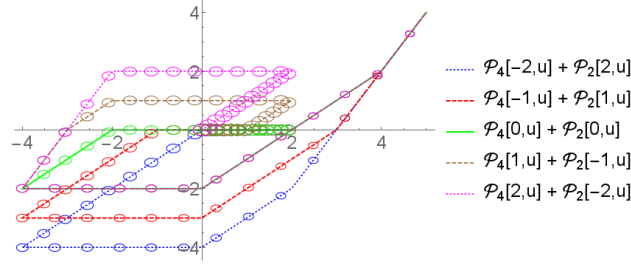
Figure 9: Input-output diagram, showing $\big(u(t), \mathcal{H}[w,u](t)\big) = \big(u(t), \mathcal{P}_4[w,u](t) + \mathcal{P}_2[-w,u](t)\big)$ for u and w as in Figure 8. The size of the circles decreases with increasing time t.

density function ρ_W of the considered random variable W:

$$\rho_W(w) = \frac{1}{C_2} \begin{cases} e^{-\frac{1}{2}r^2}, & \text{if} \quad -2 \le w \le 2, \\ 0, & \text{if} \quad |w| > 2, \end{cases} \tag{7}$$

with

$$C_2 = \int_{-2}^{2} e^{-\frac{1}{2}w^2} \, dw. \tag{8}$$

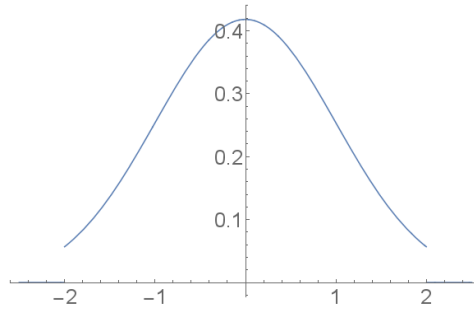The density function ρ_W is presented in Figure 10.

Figure 10: The probability density function ρ_W of the random variable W representing the initial state w.

Definition 4.1. For $w \in \mathbb{R}$, for every input function $v : [0,T] \to \mathbb{R}$ and for all $t \in [0,T]$: $\mathcal{H}[W,v] = \mathcal{P}_4[W,v] + \mathcal{P}_2[-W,v]$ denotes the random variable created as composition of the mapping $[-2,2] \ni w \mapsto \mathcal{H}[w,v] = \mathcal{P}_4[w,v] + \mathcal{P}_2[-w,v]$ with W.

Using the construction of $\mathcal{H}[W,v] = \mathcal{P}_4[W,v] + \mathcal{P}_2[-W,v]$, it holds for the expectation value and the variance:

7

$$\mathbb{E}\left(\mathcal{H}[W,v](t)\right) = \int_{-2}^{2} \mathcal{H}[w,v](t)\rho_W(w)\,\mathrm{d}w$$

$$= \int_{-2}^{2} \left(\mathcal{P}_4[w,v](t) + \mathcal{P}_2[-w,v](t)\right)\rho_W(w)\,\mathrm{d}w\,, \tag{9}$$

$$\mathsf{Var}\left(\mathcal{H}[W,v](t)\right) = \int_{-2}^{2} \left(\mathcal{H}[w,v](t) - \mathbb{E}\left(\mathcal{H}[W,v](t)\right)\right)^2 \rho_W(w)\,\mathrm{d}w$$

$$= \int_{-2}^{2} \left(\mathcal{P}_4[w,v](t) + \mathcal{P}_2[-w,v](t) - \mathbb{E}\left(\mathcal{H}[W,v](t)\right)\right)^2 \rho_W(w)\,\mathrm{d}w\,. \tag{10}$$

4.4 Example for the evolution of expectation value and variance

Considering the input function u as in Section 4.2, the evolution of u, of $\mathcal{H}[0,u] = \mathcal{P}_4[W,u](\cdot) + \mathcal{P}_2[-W,u](\cdot)$, of the expectation value $\mathbb{E}\left(\mathcal{H}[W,u](\cdot)\right) = \mathbb{E}\left(\mathcal{P}_4[W,u](\cdot) + \mathcal{P}_2[-W,u](\cdot)\right)$, and of the variance $\mathsf{Var}\left(\mathcal{H}[W,u](\cdot)\right) = \mathsf{Var}\left(\mathcal{P}_4[W,u](\cdot) + \mathcal{P}_2[-W,u](\cdot)\right)$, are presented in Figure 11. The corresponding input-output diagram for u, $\mathcal{H}[0,u] = \mathcal{P}_4[0,u] + \mathcal{P}_2[0,u]$, and $\mathbb{E}\left(\mathcal{H}[W,u](\cdot)\right) = \mathbb{E}\left(\mathcal{P}_4[W,u](\cdot) + \mathcal{P}_2[-W,u](\cdot)\right)$ are shown in Figure 12.
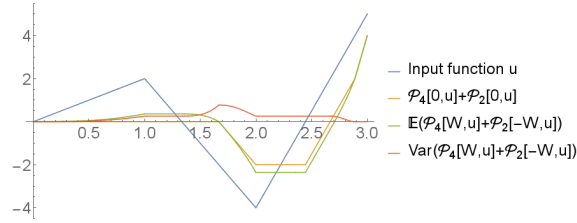

Figure 11: The evolution of the input function u, of $\mathcal{H}[0,u](\cdot) = \mathcal{P}_4[0,u] + \mathcal{P}_2[0,u]$, of the expectation value $\mathbb{E}\left(\mathcal{H}[W,u](\cdot)\right) = \mathbb{E}\left(\mathcal{P}_4[W,u](\cdot) + \mathcal{P}_2[-W,u](\cdot)\right)$, and of the variance $\mathsf{Var}\left(\mathcal{H}[W,u](\cdot)\right) = \mathsf{Var}\left(\mathcal{P}_4[W,u](\cdot) + \mathcal{P}_2[-W,u](\cdot)\right)$.

5 Model for magneto-mechanical components

In this section, results of a joined work with Daniele Davino and Ciro Visone of the Università del Sannio, Benevento, Italy, are presented. In [3, Sec. 5.1], a generalized Prandtl-Ishlinskiĭ operator (see, e.g. in [7]) is used to model the *magnetization* of Galfenol for an applied magnetic field.

Considering parameter $c_1, c_2, c_3 > 0$, the generalized Prandtl-Ishlinskiĭ operator $\Psi_{c_1,c_2,c_3} : C[0,T] \to C[0,T]$ is defined by

$$\Psi_{c_1,c_2,c_3}[H](t) := \int_{0}^{\infty} c_1 \mathrm{e}^{-r/c_2} \mathcal{P}_r[0, \tanh(c_3 H)](t)\,\mathrm{d}r\,, \quad \forall t \in [0,T],\ H \in C[0,T]. \tag{11}$$
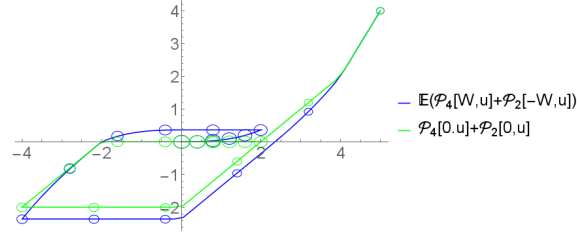
Figure 12: Input-output diagram, showing $(u(t), \mathcal{H}[0, u](t)) = (u(t), \mathcal{P}_4[0, u](t) + \mathcal{P}_2[0, u](t))$, and $(u(t), \mathbb{E}(\mathcal{H}[W, u](t))) = (u(t), \mathbb{E}(\mathcal{P}_4[W, u](t) + \mathcal{P}_2[-W, u](t)))$, for u as in Figure 11. The size of the circles decreases with increasing time t.

The values used for $c_{1,0}$ and $c_{2,0}$ in the current paper paper correspond to those used in the generalized Prandtl-Ishlinskiĭ operator in [3, Sec. 5.1] (see [2]). The parameter $c_{3,0}$ has been chosen in such that using $\Psi_{c_{1,0}, c_{2,0}, c_{3,0}}$ allows to reproduce the magnetic cycle for Galfenol at a pre-stress 39 MPa shown in [3, Figure 13], which contains only a very small hysteresis loop.

In the Figures 13–15 corresponding magnetic cycles are considered with a variation of one of the parameters c_1, c_2, or c_3. It should be noted that the the hysteresis loop is so small that the hysteresis effect can not be observed in these curves. Moreover, the variation of c_1 shown in Figure 13 and of c_2 in shown Figure 15 produce almost identical loops.
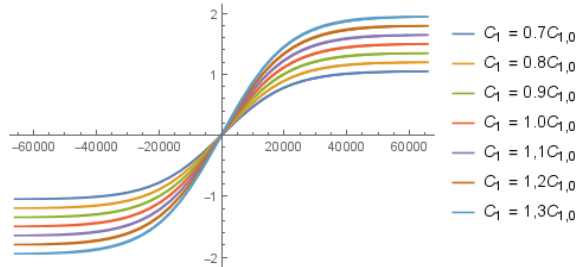

Figure 13: Input-Output diagrams, showing $(H(t), \Psi_{c_1, c_{2,0}, c_{3,0}}[H](t))$ for $c_1 \in \{0.7c_{1,0}, 0.8c_{1,0}, 0.9c_{1,0}, 1.0c_{1,0}, 1.1c_{1,0}, 1.2c_{1,0}, 1.3c_{1,0}\}$.

6 Conclusion and future work

It has been shown in some numerical examples that the output of hysteresis operators dependents on parameters within the operator, including the (internal) initial state.

First examples of considering these parameters as random variables to model uncertainties and of computing stochastic properties of the output of the model have been presented.
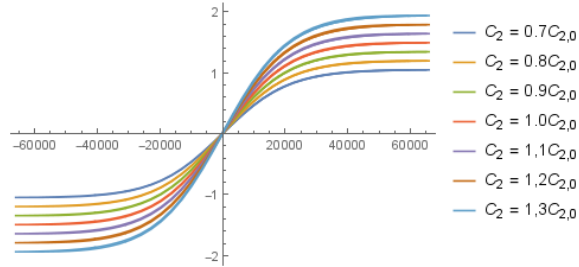
Figure 14: Input-Output diagrams, showing $\left(H(t), \Psi_{c_{1,0},c_2,c_{3,0}}[H](t)\right)$ for $c_2 \in \{0.7c_{2,0}, 0.8c_{2,0}, 0.9c_{2,0}, 1.0c_{2,0}, 1.1c_{2,0}, 1.2c_{2,0}, 1.3c_{2,0}\}$.
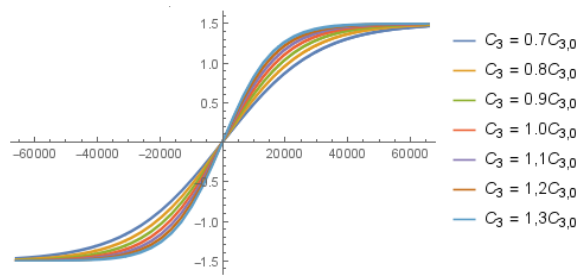

Figure 15: .

Input-Output diagrams, showing $\left(H(t), \Psi_{c_{1,0},c_{2,0},c_3}[H](t)\right)$ for $c_3 \in \{0.7c_{3,0}, 0.8c_{3,0}, 0.9c_{3,0}, 1.0c_{3,0}, 1.1c_{3,0}, 1.2c_{3,0}, 1.3c_{3,0}\}$

In the future work, in addition to the magnetic cycle, also the magneto-elastic interactions will be taken into account. It is planed to model a magnetostrictive material generating larger hysteresis loops then the one of Galfenol.

Moreover, the uncertainties in the parameters will be determined from uncertainties in the measurements, and the influence will be computed by using methods of uncertainty quantification as discussed for example in [11].

Acknowledgements

References

[1] M. Brokate and J. Sprekels. *Hysteresis and phase transitions*. Springer, New York, 1996.

[2] D. Davino. Parameters for computations. Private communication, 2016.

[3] D. Davino, P. Krejci, and C. Visone. Fully coupled modeling of magneto-mechanical hysteresis through 'thermodynamic' compatibility. *Smart Mater. Struct.*, 22(9), SEP 2013.

[4] D. Davino, P. Krejci, and C. Visone. Handling memory properties of smart materials: A review on modeling, compensation and control. In *American Control Conference (ACC)*, pages 3599–3604. IEEE, 2013.

[5] D. Davino and C. Visone. Rate-independent memory in magneto-elastic materials. *Discrete and Continuous Dynamical Systems - Series S*, 8(4):649–691, Oct 2015.

[6] G. R. Grimmett and D. R. Stirzaker. *Probability and random processes*. Oxford University Press, New York, third edition, 2001.

[7] O. Klein and P. Krejčí. Outwards pointing hysteresis operators and and asymptotic behaviour of evolution equations. *Nonlinear Anal. Real World Appl.*, 4(5):755–785, Dezember 2003.

[8] M. Krasnosel'skii and A. Pokrovskii. *Systems with Hysteresis*. Springer-Verlag, Heidelberg, 1989. Russian edition: Nauka, Moscow, 1983.

[9] P. Krejčí. *Hysteresis, Convexity and Dissipation in Hyperbolic Equations*, volume 8 of *Gakuto Int. Series Math. Sci. & Appl.* Gakkōtosho, Tokyo, 1996.

[10] I. D. Mayergoyz. *Mathematical Models of Hysteresis and their Applications*. Elsevier, second edition edition, 2003.

[11] R. C. Smith. *Uncertainty quantification: theory, implementation, and applications*, volume 12 of *Computational Science & Engineering*. Society for Industrial and Applied Mathematics (SIAM), Philadelphia, PA, 2014. Theory, implementation, and applications.

[12] A. Visintin. *Differential Models of Hysteresis*, volume 111 of *Applied Mathematical Sciences*. Springer, New York, 1994.